

## High Pressure Melting of Lithium

Anne Marie J. Schaeffer, William B. Talmadge, Scott R. Temple, and Shanti Deemyad

*Department of Physics and Astronomy, University of Utah, Salt Lake City, Utah 84112, USA*  
(Received 4 July 2012; revised manuscript received 9 August 2012; published 2 November 2012)

The melting curve of lithium between ambient pressure and 64 GPa is measured by detection of an abrupt change in its electrical resistivity at melting and by visual observation. Here we have used a quasi-four-point resistance measurement in a diamond anvil cell and measured the resistance of lithium as it goes through melting. The resistivity near melting exhibits a well documented sharp increase which allowed us to pinpoint the melting transition from ambient pressure to 64 GPa. Our data show that lithium melts clearly above 300 K in all pressure regions and its melting behavior adheres to the classical model. Moreover, we observed an abrupt increase in the slope of the melting curve around 10 GPa. The onset of this increase fits well to the linear extrapolation of the lower temperature bcc-fcc phase boundary.

DOI: [10.1103/PhysRevLett.109.185702](https://doi.org/10.1103/PhysRevLett.109.185702)

PACS numbers: 64.70.dj, 05.70.Jk, 62.50.-p

At ambient pressure, lithium is the lightest metallic element and the prototype of a simple metal, with a nearly spherical Fermi surface. The structural and electronic properties of lithium at high densities are highly counter-intuitive [1–5], and under high pressure, lithium undergoes a series of symmetry-breaking structural phase transitions [6,7]. The properties of lithium under pressure have attracted considerable attention, especially because of its possible analogy to metallic hydrogen and considerable quantum solid behavior (e.g., [8–15]). Despite a broad interest, the high pressure properties of lithium above 200 K are poorly studied. This is due to technical challenges caused by the reactivity, at high pressure and temperature, of lithium with diamond, which is the building block of static high pressure diamond anvil cells (DACs). Recent structural studies on lithium in a diamond anvil cell used x-ray diffraction to characterize the region between 77 K and room temperature at pressures up to 120 GPa. The study found that the diffraction lines had disappeared in the region between 40–60 GPa at temperatures as low as 190 K, which can be indicative of melting. This study, together with earlier high pressure melting measurements up to 15 GPa, using differential thermal analysis (DTA) in a multianvil cell [7,9,16,17], suggests a very sharp drop in the melting line between 15–40 GPa. Lithium's structure changes from fcc to lower symmetry structures in the region around 40 GPa, which according to recent molecular dynamic calculations is followed by a sharp decrease in the melting temperature to 280 K at about 60 GPa [18]. The drop in the melting temperature of lithium suggested by x-ray studies is in qualitative agreement with the molecular dynamics calculations. However, above 40 GPa, melting was observed at much lower temperatures than predicted, which has been attributed to quantum effects caused by large lattice dynamics of lithium. No prior experiments before our study have observed this drop in the melting temperature directly, and in the pressure range between  $\sim$ 15–40 GPa no experimental data have been

available [16,17,19]. Several methods have been employed to determine melting temperature at high pressure. These include differential thermal analysis, a technique suitable for larger volume pressure cells, as well as latent heat measurements, laser reflection, x-ray diffraction, discontinuity in the physical properties of the material, and visual observation of melting and crystallization [17,20,21]. Determination of the onset of melting at high pressure in a diamond anvil cell, in which the sample size is small, can be very challenging. In the particular case of lithium, which is highly reactive with diamonds at high pressures and temperatures, all previous diamond anvil cell experiments were conducted in cryostats. Those experiments conducted above room temperature were done in large volume, relatively low pressure cells. In this study for the first time we unified these two pressure and temperature ranges with a single method.

We attempted four different methods of determining the onset of melting: observation of the laser speckle pattern with simultaneous latent heat measurement, direct visual observation, and electrical resistance measurement. Of these, only the latter two methods were successful. The low melting temperature of lithium made remote temperature sensing by blackbody radiation impractical. Successful blackbody measurements are crucial to both speckle motion and latent heat methods. (Some surface effects were observed during laser heating which are explained in Supplemental Material [22].)

To collect the data presented here, we used two complementary methods. First, we used direct visual observation of the melting of lithium in an argon pressure medium below 35 GPa. Direct observation of the melting requires a relatively soft pressure medium. As lithium melts, its shape changes to minimize surface area. Determining the onset of melting visually, with a small sample, in a solid pressure medium, is difficult and susceptible to large errors. Therefore, to confirm these visual data, we used a quasi-four-probe resistance measurement to detect the

abrupt jump in electrical resistivity as the sample melts across the entire pressure range studied. The abrupt jump in the electrical resistivity of normal metals at melting has been known for a long time [23,24]. Recently, this effect has been used in a novel design to determine the melting of Au and tin in a diamond anvil cell up to 21 and 45 GPa, respectively [25,26]. However, in these measurements the circuit was optimized for reaching very high temperatures by resistive heating of a thin film of sample *in situ*, and the jump in the resistivity of the sample was a 5% effect. Using the same principle in our measurement, we used a conventional quasi-four-probe resistivity circuit that allows determination of the jump in resistivity with much higher sensitivity (Fig. 1). Detection of melting by the abrupt jump in resistivity relies upon the characteristics of the melting transition rather than upon the differences between solid and liquid phases, and so it very precisely detects the onset of melting while preventing confusion with, e.g., an amorphous phase [23,24,27,28]. The resistivity method is a tabletop experiment providing a very clear and sharp signal which is reproducible. In his paper, Mott has shown that the resistivity of normal metals just below and above their melting point approximately follows the relation  $\frac{\rho_L}{\rho_S} = e^{80L/T_M}$  [23], in which  $\rho_L$  and  $\rho_S$  are resistivities of a metal in liquid and solid phase at the melting temperature respectively,  $L$  is latent heat of fusion in kJ/mol, and  $T_M$  is

the melting temperature in degrees kelvin. The presence of a solid pressure medium allows confinement of the sample to prevent it from flowing away from the leads upon melting. This method also allows the observation of mixed solid phases and crossing of the solid-solid phase boundary in regions where structural phase transitions occur (Fig. 2). Also, this method allows estimation of the latent heat of metals at high pressure. In the presence of a solid pressure medium, which serves to confine the sample to roughly the same shape, the measured jump in resistance would be sufficient to empirically estimate the latent heat of fusion based on Mott's equation. One notable drawback to this method is that it is limited to metals.

In this Letter we present an extensive determination of the high pressure melting of lithium to 64 GPa. A sample of lithium was loaded directly onto the leads inside an argon glove box. To prevent reaction of the diamonds with the sample, a layer of alumina ( $\text{Al}_2\text{O}_3$  or LiF) of approximately  $10\ \mu\text{m}$  thickness was baked onto the diamond culets, and alumina or LiF nanopowder was used as a pressure medium. Proper baking time was necessary to remove the moisture prior to loading the lithium. No epoxy was used in the vicinity of the lithium. An insulated stainless steel gasket with a  $150\ \mu\text{m}$  hole was used in all cases. The sample was 99.9% pure lithium with a natural isotopic

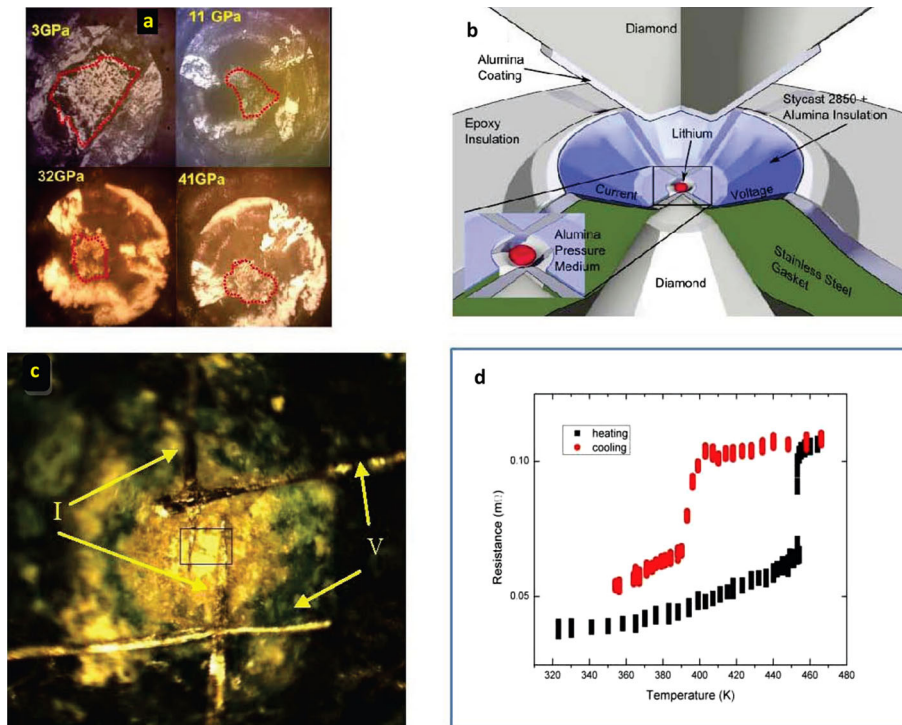


FIG. 1 (color online). (a) Micrographs of sample in reflected light. Red dotted lines are the contour of the sample. Dark spots are regions of sample or electrodes deformed under pressure and are shiny if viewed from a different angle. (b) Schematic drawing of the quasi-four-probe resistance. (c) The arrangement of electrodes prior to loading the lithium sample. The square region marks the approximate area of the sample in the measurement. (d) Large hysteresis between melting and recrystallization temperatures of a lithium sample at ambient pressure due to rapid cooling.

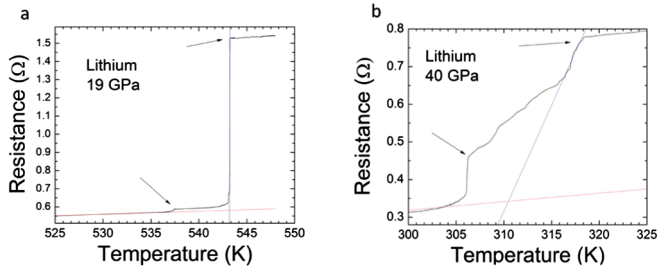


FIG. 2 (color online). Jump in resistivity at (a) 19 GPa, well within the boundaries of the fcc phase, and (b) 40 GPa, which is at the boundary of fcc and cI16. The broadening of the melting signal in the latter was reproducible, indicating the existence of mixed solid phases. The higher temperature arrow defines the completion of the melting transition and the lower temperature arrow gives the lower limit of melting. The resistances are estimated after subtraction of the lead contribution and would approximate  $L_{40\text{ GPa}} \sim 3$  kJ per mole and  $L_{19\text{ GPa}} \sim 5$  kJ per mol, using Mott's equation.

makeup (Sigma Aldrich 266000). The dimensions of the sample were approximately 50–100  $\mu\text{m}$  in diameter by 10–20  $\mu\text{m}$  thick, but varied between pressure runs. This variability, and the difficulty of determining precise sample size *in situ*, precluded measurement of the absolute resistivity of the sample; the discrete change in resistivity indicative of melting is not impacted by sample size. Pressure was calculated before and after melting by ruby scale. To enhance the signal quality and reduce the resistive heating of the sample, ac resistance measurements were done using a small current  $I_{\text{rms}} \sim 100 \mu\text{A}$ . We measured resistance with a quasi-four-probe system using Ta and Pt as electrodes and the data were collected by a lock-in amplifier (Fig. 1). The resistivity of the combined solid electrode-lithium voltage path was on the order of  $10^{-7} \Omega\text{m}$  at room temperature, with a temperature coefficient on the order of  $\sim 10^{-3} \Omega/\text{K}$ . These values were pressure dependent and also dependent on the relative dimensions of the lithium sample and the electrodes. By measurements of the relative size of the sample, including the leads in each pressure point, and comparison of our data to the theory of melting in metals, some very crude numerical estimates of the latent heat of lithium and temperature dependence of its resistivity are possible. These estimates would give a rough value of jump in resistance of lithium of about 2 times on all transitions.

Temperature was increased isobarically for each data point. The results from both of these methods, in the region they overlap, are consistent within the error (Fig. 3). The temperature of the whole DAC was controlled in two ways. Near room temperature, a homemade ceramic oven resistively heated the DAC and was initially precooled with a dry ice bath. The DAC was heated at a rate slow enough to avoid thermocouple delay ( $\sim 0.5$  K/min). Between 77 and 325 K, the DAC was cooled with liquid nitrogen

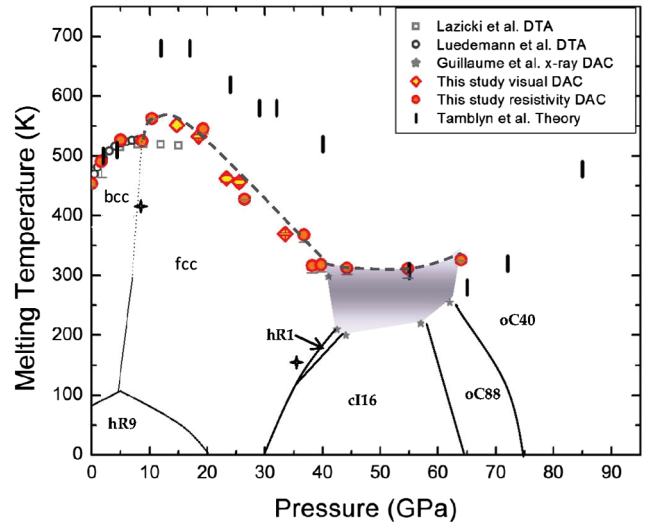


FIG. 3 (color online). The melting curve of lithium [7,9,16]. Solid lines represent the boundaries of solid structures determined by x-ray diffraction [6,7]. The dotted line is the interpolated bcc-fcc phase boundary. The dashed line is to guide the eye along the melting curve of lithium. The shaded area is the region below the melting curve in which x-ray diffraction lines disappear in condensed lithium. Pressure uncertainties are  $\pm 1$  GPa. Slope changes at 9 and 35 GPa represent small but clear change in the resistance versus temperature (+).

in a cryostat and data collected during passive warming ( $< 0.2$  K/min). The temperature in both cases was recorded on the gasket surface.

One of the problems in high pressure and temperature studies of lithium is its high chemical reactivity. Lithium reacts with diamond at elevated pressures, which leads to failure of the experiment and the diamonds. Several methods have been employed to minimize this reactivity, including limiting the studies to lower temperatures typically below 200 K. This would not be suitable for completing the phase diagram from 15–30 GPa based on previous studies [7,16,19]. Lithium can flow through small cracks at high pressure, and a sufficiently thick layer of nonreactive pressure medium is required to protect the diamonds and preserve sample purity. To maintain the purity of the lithium sample in our experiments, we separated the lithium from both diamond anvils by nonreactive pressure transmitting media. In the two different parts of this study, by visual observation and electrical resistivity, argon, alumina, and LiF were used as pressure transmitting media. LiF is nonreactive with lithium. At ambient pressure, argon and alumina do not react with lithium to the highest temperatures of this study ( $< 600$  K). We excluded the possibility of any reaction between alumina, argon, and LiF at high pressure and confirmed the lack of any reaction between the diamonds and the sample by several observations. (a) Lithium remained shiny throughout both resistivity and visual observation experiments and no sign of darkening, change of color, or loss of metallic luster was

observed over long periods of data collections (Fig. 1). Data were collected in five separated runs, each lasted anywhere from two to seven days. (b) The diamonds remained intact after completing each pressure run and were reused. (c) Some of the ruby spheres ( $\text{Cr}^+$  doped  $\text{Al}_2\text{O}_3$ ) that were used to measure the pressure were embedded in the sample, and all of them remained active. (d) After cooling, the electrical resistance of the sample returned to the initial value at lower temperatures. This, however, required several hours of annealing to recover the sample from cold working. (e) The discontinuity at electrical resistivity was observed at the same temperature for a given pressure and was reproducible. (f) While there was hysteresis between melting and recrystallization, melting occurred consistently at the same temperature. The recrystallization temperature was highly dependent upon the rate of cooling, and in all instances recorded, it was lower than the melting temperature. This difference between the melting and recrystallization temperatures of lithium have been reported previously at ambient pressure [16] and is observed in many materials due to cold working [29–31]. (g) Consistent melting data points have been taken in random pressure order during several runs, in one of which the sample was kept in a cryostat and below room temperature during the entire run. (h) During resistivity measurements we once cooled the sample to 4 K and measured its superconductivity at 45 GPa, which was consistent with previous electrical resistivity measurements on lithium [2]. (i) The resistivity measurement resulted in consistent melting temperatures for both LiF and alumina as the pressure medium.

In this study, we measured the melting line of lithium up to 64 GPa and observed several new phenomena (Fig. 3). At about 10 GPa, we observed a jump in the melting temperature which may be indicative of a structural phase transition from bcc-fcc; this change agrees with the Clausius-Clapeyron relation, as the fcc phase is denser than the bcc phase. The melting temperature decreased monotonically and very quickly between 11–40 GPa, going from 535 to 310 K, in qualitative agreement with previous interpolations. This rapid decrease in melting temperature is consistent with theory, and may be indicative of the onset of a symmetry-breaking phase transition from fcc to a lower symmetry phase. The melting temperature showed a very flat landscape between 40–64 GPa and reached a minimum of 306 K at about 44 GPa. We did not observe any indication of melting below room temperature down to 77 K at any pressure, and the resistivity of the sample between 77–279 K had a nearly linear temperature dependence in all pressures (Fig. 4). At two pressures, 19 and 35 GPa, an obvious change in slope was observed (Fig. 3, inset). This change in slope in both cases is seen at pressures and temperatures very near solid-solid phase boundaries. We did not observe any obvious change in slope in the range of 200 K between 40 and 60 GPa, which

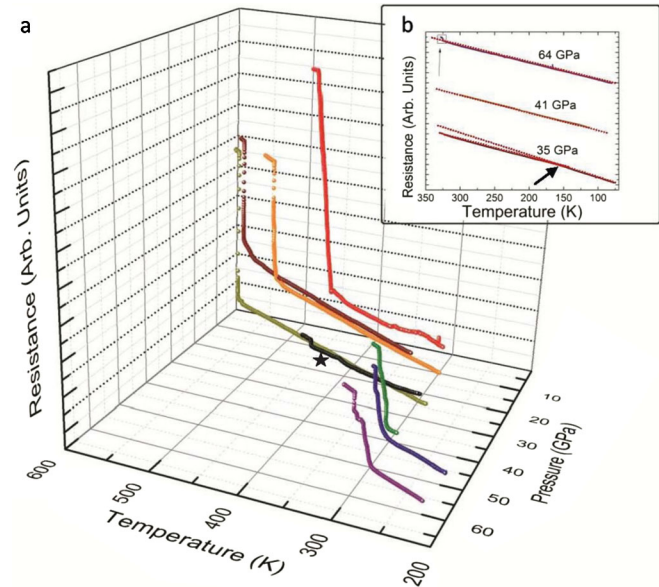


FIG. 4 (color online). (a) The resistance of lithium at different pressures. The sample size was smaller in the run shown by the black curve marked with a star in which the jump in the resistivity is proportionally smaller. (b) The resistance versus temperature from room temperature to 77 K at 35, 41, and 64 GPa. Melting at 64 GPa was observed above room temperature inside the cryostat (see arrow); melting at 35 and 41 GPa was measured in the homemade oven outside of the cryostat (see text). Red dotted lines in the subset graph are linear guidelines. A change in slope is observed at 35 GPa. Arrow in the subset graph points to the change in slope at 35 GPa near the boundary of fcc-CI16/hR1 phases.

would indicate a change in phase at the previously reported “cold melting” region. Our experimental limitation in determining the absolute value of the resistivity of lithium in the present experiments does not allow us to estimate the pressure dependence of the resistivity of lithium on a high temperature isotherm. A four-probe resistivity measurement at room or higher temperature would provide insight to the electronic properties of this phase.

We observed a large contrast between our melting temperatures above 40 GPa with earlier results on the melting curve of lithium using an x-ray diffraction technique [7]. Above 40 GPa, lithium undergoes several symmetry-breaking structural phase transitions to low symmetry phases and the x-ray studies on the sample are very challenging. Loss of solid x-ray diffraction peaks is not a proof of melting if the liquid peaks are not observed, which is the case for the previously reported melting line ([7], Methods section). One possibility is that the lithium in these x-ray studies has been supercooled to form a glassy, or highly disordered, phase due to cold working. Information on the thermodynamic paths of the sample is necessary to rule out this possibility. While detailed information is not provided in the previous x-ray studies about the thermodynamics paths of the sample, it has been specified that the sample

has been mainly kept below 200 K and in some instances data could have been collected at 300 K for 2–3 h, which may not be sufficient time for annealing the sample. Cold working can cause a drop in the recrystallization temperature, and in lithium we could show a very large effect at ambient pressure by rapid cooling of the sample [Fig. 1(d)]. Recrystallization temperature ( $T_{RC}$ ) is not a fixed temperature like melting point temperature ( $T_m$ ), and in pure metals it can be as low as  $T_{RC} = 0.4T_m$  [32]. The recrystallization behavior depends on several variables, including temperature, time, initial grain size, and amount of recovery or polygonization prior to the start of recrystallization [32], and the extent that material is cold worked can be substantial in high pressure experiments.

In conclusion, the result of this study does not support any drastic effect on the melting temperature due to lattice quantum effects at any pressure, in contrast to previous x-ray experiments [7]. Our results, however, do not exclude the importance of lattice quantum dynamics, which are present in both liquid and solid phases, to the high pressure properties of lithium.

The authors would like to acknowledge the generous donation of some of the major equipment used in this study by Linda and Robert Grow from UPRI Co. The authors would like to thank Dr. Eugene Mishchenko for insightful discussions on the topic of melting and reviewing this manuscript, Matthew DeLong for providing technical and intellectual support in design of the experiment, and the University of Utah UROP fund for partial financial support.

- 
- [1] T. Matsuoka and K. Shimizu, *Nature (London)* **458**, 186 (2009).
- [2] K. Shimizu, H. Ishikawa, D. Takao, T. Yagi, and K. Amaya, *Nature (London)* **419**, 597 (2002).
- [3] V. V. Struzhkin, M. I. Erements, W. Gan, H.-k. Mao, and R. J. Hemley, *Science* **298**, 1213 (2002).
- [4] S. Deemyad and J. S. Schilling, *Phys. Rev. Lett.* **91**, 167001 (2003).
- [5] J. Tuoriniemi, K. Juntunen-Nurmilaukas, J. Uusvuori, E. Pentti, A. Salmela, and A. Sebedash, *Nature (London)* **447**, 187 (2007).
- [6] M. Hanfland, K. Syassen, N. E. Christensen, and D. L. Novikov, *Nature (London)* **408**, 174 (2000).
- [7] C. L. Guillaume, E. Gregoryanz, O. Degtyareva, M. I. McMahon, M. Hanfland, S. Evans, M. Guthrie, S. V. Sinogeikin, and H. K. Mao, *Nature Phys.* **7**, 211 (2011).
- [8] J. B. Neaton and N. W. Ashcroft, *Nature (London)* **400**, 141 (1999).
- [9] A. Lazicki, Y. Fei, and R. J. Hemley, *Solid State Commun.* **150**, 625 (2010).
- [10] F. A. Gorelli, S. F. Elatresh, C. L. Guillaume, M. Marqués, G. J. Ackland, M. Santoro, S. A. Bonev, and E. Gregoryanz, *Phys. Rev. Lett.* **108**, 055501 (2012).
- [11] A. F. Goncharov, V. V. Struzhkin, H.-k. Mao, and R. J. Hemley, *Phys. Rev. B* **71**, 184114 (2005).
- [12] C. Filippi and D. M. Ceperley, *Phys. Rev. B* **57**, 252 (1998).
- [13] J.-Y. Raty, E. Schwegler, and S. A. Bonev, *Nature (London)* **449**, 448 (2007).
- [14] S. Stishov, *Phys. Usp.* **44**, 285 (2001).
- [15] T. H. Lin and K. J. Dunn, *Phys. Rev. B* **33**, 807 (1986).
- [16] H. D. Luedemann and G. C. Kennedy, *J. Geophys. Res.* **73**, 2795 (1968).
- [17] R. Boehler, *Phys. Rev. B* **27**, 6754 (1983).
- [18] I. Tamblyn, J.-Y. Raty, and S. A. Bonev, *Phys. Rev. Lett.* **101**, 075703 (2008).
- [19] A. Lazicki, R. J. Hemley, W. E. Pickett, and C.-S. Yoo, *Phys. Rev. B* **82**, 180102 (2010).
- [20] S. Deemyad, E. Sterer, C. Barthel, S. Rekhi, J. Tempere, and I. F. Silvera, *Rev. Sci. Instrum.* **76**, 125104 (2005).
- [21] P. W. Bridgman, *Phys. Rev.* **27**, 68 (1926).
- [22] See Supplemental Material at <http://link.aps.org/supplemental/10.1103/PhysRevLett.109.185702> for an explanation of the change in the appearance of the lithium detected at high pressure and temperature, which was dependent on its thermal history.
- [23] N. F. Mott, *Proc. R. Soc. A* **146**, 465 (1934).
- [24] T. C. Chi, *J. Phys. Chem. Ref. Data* **8**, 339 (1979).
- [25] S. T. Weir, M. J. Lipp, S. Falabella, G. Samudrala, and Y. K. Vohra, *J. Appl. Phys.* **111**, 123529 (2012).
- [26] S. T. Weir, D. D. Jackson, S. Falabella, G. Samudrala, and Y. K. Vohra, *Rev. Sci. Instrum.* **80**, 013905 (2009).
- [27] D. Errandonea, *J. Appl. Phys.* **108**, 033517 (2010).
- [28] A. M. Rosenfeld and M. J. Stott, *Phys. Rev. B* **42**, 3406 (1990). J. Konys and H. U. Borgstedt, *J. Nucl. Mater.* **131**, 158 (1985).
- [29] F. C. Campbell, *Elements of Metallurgy and Engineering Alloys* (ASM International, Materials Park, OH, 2008).
- [30] T. Schenk, D. Holland-Moritz, V. Simonet, R. Bellissent, and D. M. Herlach, *Phys. Rev. Lett.* **89**, 075507 (2002).
- [31] D. Turnbull, *J. Appl. Phys.* **21**, 1022 (1950).
- [32] W. D. Callister and D. G. Rethwisch, *Fundamentals of Materials Science and Engineering: An Integrated Approach* (John Wiley and Sons, New York, 2001).